



Published in final edited form as:

*Surgery*. 2018 August ; 164(2): 262–273. doi:10.1016/j.surg.2018.03.008.

## GDF11 induces kidney fibrosis, renal cell epithelial-to-mesenchymal transition and kidney dysfunction and failure

Marianne Pons, PhD<sup>1</sup>, Leonidas G. Koniaris, MD<sup>1</sup>, Sharon M. Moe, MD<sup>2,3</sup>, Juan C. Gutierrez, MD<sup>4</sup>, Aurora Esquela-Kerscher, PhD<sup>5</sup>, and Teresa A. Zimmers, PhD<sup>1,6,7</sup>

<sup>1</sup>Department of Surgery, Indiana University School of Medicine

<sup>2</sup>Department of Medicine, Indiana University School of Medicine

<sup>3</sup>Roudebush Veterans Administration Medical Center

<sup>4</sup>Department of Surgery, University of Miami School of Medicine

<sup>5</sup>Department of Microbiology and Molecular Cell Biology, Eastern Virginia Medical School

<sup>6</sup>Departments of Anatomy and Cell Biology, Biochemistry and Molecular Biology and Otolaryngology—Head & Neck Surgery, Indiana University School of Medicine

<sup>7</sup>IU Simon Cancer Center

### Abstract

**Introduction**—GDF11 modulates embryonic patterning and kidney organogenesis. Herein, we sought to define GDF11 function in the adult kidney and in renal diseases.

**Methods**—In vitro renal cell lines, genetic and murine in vivo renal injury models were examined.

**Results**—Among tissues tested, Gdf11 was highest in normal adult mouse kidney. Expression was increased acutely following 5/6 nephrectomy (5/6Nx), ischemia-reperfusion injury, kanamycin toxicity or unilateral ureteric obstruction (UUO). Systemic, high-dose GDF11 administration in adult mice led to renal failure, with accompanying kidney atrophy, interstitial fibrosis, epithelial-to-mesenchymal transition (EMT) of renal tubular cells, and eventually death. These effects were associated with phosphorylation of SMAD2 and could be blocked by Follistatin. In contrast, Gdf11 heterozygous mice showed reduced renal Gdf11 expression, renal fibrosis and expression of fibrosis-associated genes both at baseline and after UUO compared with wild-type littermates. The kidney-specific consequences of GDF11 dose modulation are direct effects on kidney cells. GDF11 induced proliferation and activation of NRK49f renal fibroblasts and also promoted EMT of IMCD-3 tubular epithelial cells in a SMAD3-dependent manner.

---

**Corresponding authors:** Teresa A. Zimmers, Ph.D. and Leonidas G. Koniaris, M.D. 980 W. Walnut Street, R3-C518, Department of Surgery, Indiana University School of Medicine, Indianapolis, IN 46202, zimmerst@iu.edu and lkoniar@iu.edu, Phone: 317.278.7289.

**Publisher's Disclaimer:** This is a PDF file of an unedited manuscript that has been accepted for publication. As a service to our customers we are providing this early version of the manuscript. The manuscript will undergo copyediting, typesetting, and review of the resulting proof before it is published in its final citable form. Please note that during the production process errors may be discovered which could affect the content, and all legal disclaimers that apply to the journal pertain.

**Conclusions**—Taken together, these data suggest that GDF11 and its downstream signals are critical in vivo mediators of renal injury. These effects are through direct actions of GDF11 on renal tubular cells and fibroblasts. Thus, regulation of GDF11 presents a therapeutic target for diseases involving renal fibrosis and impaired tubular function.

### Keywords

acute kidney injury; fibrosis; GDF-11 or GDF11; TGF- $\beta$ ; fibroblast; epithelial-to-mesenchymal transition; nephrectomy; obstructive nephropathy; genetically engineered mouse model

---

## INTRODUCTION

The TGF- $\beta$  super family and its signaling pathways have been implicated in many aspects of kidney organogenesis, growth regulation, and pathophysiology. TGF- $\beta$  itself is a key regulator of both acute and chronic kidney injury. TGF- $\beta$  induces expression of fibrotic genes and mediates glomerular and tubular cell apoptosis and epithelial-to-mesenchymal (EMT) cell transition, the mechanism by which tubular epithelial cells may acquire a myofibroblastic phenotype essential for the pathogenesis of fibrosis<sup>1–6</sup>. In addition to TGF- $\beta$ , the related ligand activin<sup>7–11</sup>, its inhibitor follistatin<sup>12–15</sup>, TGF- $\beta$  and activin receptors<sup>16,17</sup>, and downstream signaling partners, the SMAD proteins<sup>18, 19</sup>, have been implicated in kidney development, injury and disease.

The TGF- $\beta$  family member, growth/differentiation factor-11 (GDF-11/GDF11, also called BMP-11), remains incompletely understood<sup>20–25</sup>. Essential roles for this protein in embryonic patterning and development<sup>20, 26–28</sup>, as well as kidney organogenesis<sup>20, 29</sup>, have been demonstrated using targeted deletion of *Gdf11*. Indeed, the majority of *Gdf11* null mice exhibit bilateral kidney agenesis<sup>29</sup>.

GDF11's functions in the adult animal are highly controversial<sup>30</sup>. Recent studies report that circulating GDF11 declines in age and that GDF11 supplementation reverts the aging phenotype in heart, muscle and brain in mice<sup>31–34</sup>. Using similar approaches, other labs report null or opposite results, provoking fierce debate<sup>30, 35–39</sup>. Given these conflicting studies, currently both the essential, non-redundant roles of GDF11 in the adult and the consequences of sustained administration are unknown. .

GDF11 exerts its developmental effects at least in part by binding TGF- $\beta$ /activin receptors type I (TGFBR1/ALK5)<sup>42</sup> and type II (ACVR2A, ACVR2B)<sup>43</sup>. Receptor binding stimulates intrinsic serine-threonine kinase activity and induces phosphorylation and nuclear translocation of SMAD proteins, downstream transcription factors<sup>44, 45</sup>. Because of its essential role in kidney development and the reported roles of ALK5, ACVR, and SMAD in kidney disease, we hypothesized that GDF11 might also play an important role in adult kidney. Herein, we show essential non-redundant roles for GDF11 in mediating kidney injury and fibrosis, along with detrimental-effects of exogenous GDF11 on renal function. Studies in cell culture suggest these effects are direct actions of GDF11 on renal fibroblasts and tubular epithelial cells.

## MATERIALS AND METHODS

### Materials

Diuresis and urine collection were performed in Nalgene metabolic cages (Nalge Nunc, Rochester, NY). Antibodies used were  $\alpha$ -SMA, vimentin, E-cadherin (Sigma, St Louis, MO), SMAD2, pSMAD2 (Cell Signaling Technology, Beverly, MA), PCNA (Santa Cruz Biotechnology, Santa Cruz, CA), collagen type I, collagen type IV (Biodesign International, Saco, ME), and Alexa Fluor 488 (Molecular Probes, Eugene, OR). Western blotting was done using HRP-conjugated secondary antibodies and SuperSignal West Pico or Femto (Pierce, Rockford, IL). Immunohistochemical staining was done using Vectastain (Vector Laboratories, Burlingame, CA) and DakoCytomation kits (DAKO, Carpinteria, CA). DNA was purified with Puregene® Genomic DNA Purification Kit (Gentra Systems, Minneapolis, MN). Primers were obtained from Sigma Genosys (St. Louis, MO).

### Mice

Athymic nu/nu mice were purchased from Harlan (Indianapolis, IN). Male C57BL/6J used in 5/6 nephrectomy experiments were originally obtained from The Jackson Laboratories (Bar Harbor, ME). Male C57BL/6J mice (8–10 weeks old) were used for characterization of *Gdf11* expression after kidney injury. Female athymic nu/nu mice were used for cell injections. C57:Gdf11<sup>tm1Lee</sup> mice were generated by crossing Gdf11<sup>+/-</sup> females to C57BL/6J males. Genotyping was by PCR on tail DNA as described<sup>29</sup>. All experiments were performed according to the guidelines of the Institutional Animal Care and Use Committees at University of Miami or Indiana University School of Medicine. Mice were housed in a temperature-controlled, 12-hour light/dark photocycle and maintained on a standard rodent diet with free water and food access. Surgical procedures were performed on 8–12 week-old male mice under isoflurane general anesthesia using a non-rebreathing apparatus on a heated re-circulating water bed. Buprenorphine (0.05 mg/kg) was given by intramuscular injection once daily for 3 d after surgery for pain control. Unilateral ureteric obstruction was performed by midline incision and gentle manipulation of the abdominal contents to reveal the right ureter, which was then tied twice with sutures. Subtotal nephrectomy was performed by ligation and removal of one kidney and resection of 2/3 of the remaining kidney on the same day. Kanamycin (360 g/kg) was delivered in a single intraperitoneal (i.p.) injection.

For GDF11 administration, a Chinese Hamster Ovary (CHO) cell line stably producing GDF11 (CHO-GDF11) was obtained by introduction of the plasmid vector pMSXND containing full-length *Gdf11* cDNA into DHFR-deficient CHO-DUXX cells by protoplast fusion and subsequent methotrexate selection. A similarly-selected CHO cell line (CHO-control) not expressing detectable recombinant protein was used as a control. Female athymic nude mice (6–8 weeks old) were i.m.-injected in the upper rear leg with either CHO-GDF11 cells or CHO-control cells in 0.1 mL PBS. For delivery of recombinant GDF11 (R&D Systems, Minneapolis, MN), C57BL/6J male mice (8 wks) were implanted with 7-day Alzet osmotic pumps in the peritoneum. Controls received pumps filled with saline. For all experiments, blood and tissue was collected under general anesthesia at time of euthanasia. Water content of carcasses and kidneys was determined by calculating the

difference in mass before and after oven-drying. All in vivo studies with cell lines were repeated >4 times with at least 8 mice per group.

### Serum and urine chemistry

Urine osmolalities were measured using a freezing-point depression osmometer using a modified Jaffe method. Total protein in urine was measured using the Coomassie Plus™ Bradford Assay. BUN, creatinine, sodium, potassium, and phosphorus levels in serum were measured on an autoanalyzer. Creatinine clearance was calculated using 24 hour samples.

### Histology and morphometry

Formalin-fixed, paraffin-embedded kidneys were cut into 5- $\mu$ m sections onto glass slides and stained with hematoxylin and eosin (H&E), Periodic Acid Schiff, immunohistochemistry, Masson's Trichrome, or Sirius Red. Quantification of collagen was performed using Photoshop CS (Adobe, San Jose, CA) to color threshold with ImageJ (NIH, Bethesda, MD). Each measurement was from ten randomly chosen, non-overlapping 400X fields per treatment group ( $n = 4$ ). For morphometry, the surface area of 40 glomeruli and 80 tubules per mouse were measured on Periodic Acid Schiff-stained kidney sections at day 12 using an Olympus BH-2 microscope (Shinjuku, Tokyo), a Micro Image A209RGB color video camera, and MetaMorph 4.5 (Universal Imaging Co., West Chester, PA). Because subcapsular and juxtamedullary glomeruli differ in size, glomeruli were randomly selected in each section as they were encountered between the capsule and the juxtamedullary region. The same approach was used to select transverse sections of the tubules. In situ hybridization for *Gdf11* was done essentially as described<sup>46</sup> using digoxigenin-labeled riboprobes on frozen sections. The riboprobes used for the *Gdf11* transcript corresponded only to the pro-region and the 3' UTR in order to avoid cross-hybridization to myostatin.

### Western blotting analysis

Individual kidney samples were homogenized in RIPA buffer with and centrifuged. Protein concentrations were determined using the Coomassie Plus Bradford Assay Kit (Pierce, Rockford, IL). Total kidney protein content was calculated using starting kidney weight multiplied by measured milligrams of protein per gram of kidney weight. Blots of at least 4 individual mice per group and time point were performed. For blots presented, equivalent amounts of protein from individual kidney samples were pooled at each time point, each representing 3–4 individual kidneys. Samples were suspended in Laemmli loading buffer and boiled for 5 min, then subjected to SDS-PAGE on 10.5–14% gradient gels. Chemiluminescent signals were detected by exposure to Kodak BioMax Light film (Rochester, NY). Bands were analyzed by densitometry using ImageJ 1.30 software. Ponceau-S staining was used as a loading control.

### Northern blot and qRT-PCR

Total RNA was extracted from TRIzol (Fischer Scientific). Northern blot of total or twice poly(A)<sup>+</sup>-selected RNA was performed as described<sup>47</sup>. Primer 3 was used on the *Gdf11* mRNA sequence XM-125935 to design the optimal intron-spanning primer pair, 5'-AGGACTTCTTGGAAGAGGACGAG-3' and 5'-CCTTGGGGCTGAAGTGAAA-3', for

an amplicon of 129 bp. Other primer pairs used are described in Table 2. Reverse transcription was performed using random primers on 1.25 µg total RNA using a High-Capacity cDNA Archive Kit (Applied Biosystems–Life Technologies, Carlsbad, CA). PCR reactions were performed using the TaqMan Universal Master Mix (Applied Biosystems–Life Technologies) or the iQ™ SybrGreen Supermix (BioRad Laboratories, Hercules, CA) per manufacturer’s instructions. The amplification program consisted of 1 cycle at 95°C for 10 min (hot start), followed by 40 cycles of 95°C for 15 s and 65°C for 1 min. PCR products were analyzed on ethidium bromide-stained 2% agarose gels to verify the specificity of PCR amplification, and melting curves and standard curves were obtained for each primer pair on normal kidney cDNA. Six replicates were performed for each experimental sample. Each sample was normalized to *18S rRna* or *Gapdh* transcripts. Relative changes in gene expression were quantified using the  $2^{-CT}$  method<sup>48</sup>.

### Cell culture

NRK49f, NRK52e, HK-2, and IMCD-3 cell lines were purchased from ATCC (Manassas, VA). For proliferation studies, NRK49f cells were seeded in 96-well plates in media containing recombinant GDF11 or TGF-β (R & D Systems) and incubated for 5 d. A MTT assay was used to measure cell viability. For bright-field morphological analysis and preparation of Western blot and PCR extracts, cells were grown in plastic dishes. For αSMA immunohistochemistry and immunofluorescence of SMAD2, E-cadherin, vimentin and αSMA, cells were grown in chamber slides (Nalge Nunc). For immunofluorescence, cells were visualized on a Zeiss LSM510/UV confocal microscope. Inhibitors were added simultaneously with 50 ng/mL GDF11 as follows: 50 ng/mL follistatin (R&D Systems), 500 ng/mL SB-431542 (Sigma), and 10 µM SIS3 (Calbiochem–EMD Millipore, Darmstadt, Germany).

### Statistical analysis

All in vivo results shown are representative of experiments performed at least thrice. In vitro data were performed at least twice. All data are presented as mean ± SEM. Data were analyzed for significance using unpaired two-tailed Student’s t-test or one-way ANOVA with Tukey-Kramer multiple comparisons post-test for groups larger than two.  $P < 0.05$  was considered significant.

## RESULTS

### GDF11 expression is increased in adult mouse kidney following acute kidney injury

Northern blot analysis detected two GDF11 mRNA transcripts (~4.2 kb and 3.2 kb) in multiple adult mouse tissues, although expression was most prominent in the kidney and brain (Figure 1A). In situ hybridization for GDF11 expression in the post-natal kidney was difficult due to low signal nonetheless it demonstrated staining in distal tubules, cortical collecting ducts, and medullary rays (Figure 1B). We then examined GDF11 in commonly used mouse models of acute kidney injury (AKI). First, 5/6 nephrectomy (5/6Nx, removal of one kidney in total and 2/3 of the other), induces AKI within 10–12 days after injury, followed by modest compensatory hypertrophy affecting most components of the residual nephrons<sup>49, 5051</sup>. Northern blot analysis of mRNA from remnant kidneys following 5/6Nx

revealed increased *Gdf11* expression as early as 6–12 h (Figure 1C). Second, kanamycin intoxication was used to induce extended cortical necrosis and acute tubular necrosis, which is typically followed by compensation, tissue repair, and regeneration. Indeed, *Gdf11* expression was increased in the kidneys of mice treated with a single dose of kanamycin (Figure 1C), demonstrating similar timing as for the subtotal nephrectomy (Figure 1D). Third, unilateral ureteric obstruction (UUO) is a model of progressive obstructive nephropathy, marked by profound cortical ballooning and fibrosis. Quantitative rtPCR (qPCR) demonstrated a 3–6-fold induction of *Gdf11* (Figure 1E) in the obstructed kidney after UUO. These results suggest that kidney injury of different etiologies leads to increased GDF11.

### **Exogenous GDF11 administration induces kidney injury and urine concentrating defects**

—To study whether GDF11 increases in kidney injury might be pathogenic or compensatory in response to injury, we delivered GDF11 by injecting CHO cells expressing recombinant GDF11 (CHO-GDF11) into the thigh of athymic nude mice. Similarly-selected cell lines not expressing exogenous secreted protein were used as controls. Previous studies in our laboratory have used a similar approach to identify biological activities for various secreted proteins<sup>52–60</sup>, including the closely related myostatin. GDF11-treated mice gradually lost weight and by 12 days exhibited a hunched posture and lethargy consistent with uremia. GDF11-treated mice developed severe acute kidney injury with elevated BUN, creatinine, phosphorus and reduced creatinine clearance (Figure 2 and Table 1). These mice had polyuria and low urine osmolarity despite similar serum sodium and osmolarity, indicative of a urinary concentrating defect (Table 1). The decreased kidney function (increased BUN and creatinine) in GDF11-treated mice did not reflect volume depletion due to the polyuria, as GDF11-treated mice had appropriate increase in water intake. Moreover, GDF-11-treated and control mice had statistically indistinguishable total body water content (GDF11: 45.7% ± 2.3% vs Control: 40.35% ± 4.3%, n = 3 per group, *NS*). Weight loss, kidney dysfunction, and death were specific to GDF-11 expression because these effects were not observed in CHO-control mice (Figure 2A–D and Table 1) or in mice injected with other CHO cell lines expressing recombinant proteins including GDF-1, GDF-2, GDF-10, follistatin, IL-6, or myostatin pro-peptide (not shown).

Similar, although less dramatic results were observed using recombinant GDF11 delivered to C57BL/6 male mice via osmotic minipumps. GDF11 (10 µg over 7d) induced a rise in BUN over carrier-treated mice (GDF11: 41.25 ± 3.326 vs. carrier: 26.50 ± 2.958; n = 4 per group, *P* < 0.02) and weight loss of 7.89% ± 2.76% (*P* < 0.05) versus carrier controls, suggesting effects in the CHO-GDF11 mice were due to GDF11 and not other properties of the cells.

### **Exogenous GDF11 induced kidney injury with protein loss, tubular proliferation and fibrosis**

At necropsy, kidney mass from CHO-GDF11 mice was significantly reduced compared with controls. In a time-course analysis, more prolonged GDF11 treatment led to progressive declines of kidney mass and reduced total kidney protein (Figure 3 A and B). However total kidney water and mRNA content were unchanged while DNA content was increased (Figure

3C). Histology showed the primary abnormality in GDF11 treated mice was atrophy of the tubular epithelial cells, which demonstrated relatively scant cytoplasm (Figure 3D). Overall kidneys from GDF11-treated mice showed medullary atrophy and cortical thinning with a reduction in tubule area, although glomerular area was unchanged (Figure 3E).

Reduced kidney mass was apparently due to loss of protein and not cell death. There was no evidence for tubular cell apoptosis histologically (Figure 3D) or by caspase-3 activity or caspase -3 cleavage by Western blotting (data not show). There was, however, evidence of cell proliferation. Proliferating Cell Nuclear Antigen (PCNA)-positive cells along with mitotic figures were observed in the interstitium, glomeruli, and tubular epithelium, indicating that GDF11 induced cellular proliferation (Figure 3F), with the majority of labeled cells being tubular epithelial cells. This was not a late effect of GDF11, given that PCNA levels were increased in total kidney extract as early as 3d after onset of treatment (Figure 3F). Consistent with cell proliferation induced by GDF11, total kidney DNA also increased (GDF11:  $2.25 \pm 0.131$  mg,  $n = 12$  vs. Control:  $1.63 \text{ mg} \pm 0.099$ ,  $n = 12$ ,  $P < 0.001$ ).

Evidence of fibrosis and epithelial-to-mesenchymal transition (EMT) was also noted. Sirius red, Masson's trichrome staining and collagen immunohistochemistry revealed significantly increased collagen deposition in the renal cortex of GDF11-treated mice (Figure 4A, B). QPCR assay results were consistent with histological results, showing that GDF11 treatment increased expression of collagen precursors *Coll1a1*, *Coll3a1*, *Coll4a3*, and the pro-fibrotic TGF- $\beta$  (Figure 4D). Expression of the epithelial marker *E-cadherin* was reduced (Figure 4D), while staining for vimentin, a mesenchymal marker<sup>46</sup>, appeared in the tubular epithelium of GDF11-treated kidneys but not controls (Figure 4C).

### **GDF11-induces kidney injury associated with activation of pSMAD2 and was blocked by Follistatin**

Genetic and biochemical data indicate that GDF11 binds and activates a TGFBR1/ALK5 and ACVR2b complex that typically signals through phosphorylation of SMAD2/3 and association with SMAD4<sup>61</sup>. Consistent with GDF11 activation of these pathways in renal cells, GDF11 treatment induced SMAD2 phosphorylation in mouse kidneys. Western blot analysis revealed increased phosphorylation of SMAD2 with GDF11 treatment, evident as early as 3 d post-injection and in all GDF11-treated kidney samples (Figure 5A).

Immunohistochemistry revealed increased overall pSMAD2 staining, as well as an increased fraction of positive-staining tubular epithelial cells (but not glomerular cells) in GDF11-treated kidneys (Figure 5B). This distribution is consistent with the known expression pattern of TGFBR1/ALK5 and ACTRIIB/ACVR2B in tubular cells<sup>14</sup>. We then examined the ability of follistatin, an inhibitor of both myostatin and GDF11 receptor binding<sup>14, 15, 54, 62</sup>, to block CHO-GDF11-induced kidney failure. We injected control or follistatin expressing cells into a contralateral leg from the GDF11 secreting cells. Such dual administration of CHO-GDF11/ CHO-follistatin cells doubled survival time (to moribund) as compared to CHO-GDF11/CHO-controls (Figure 5C). These results suggest that GDF11 acts by receptor binding and direct activation of the SMAD2/3 pathway in the kidney and not indirectly as a consequence of effects on other tissues.

## Reduced GDF11 expression leads to reduced fibrosis after UUU

*Gdf11* expression was increased after fibrotic injury induced by unilateral ureteric obstruction (Figure 1E). We tested whether reduced GDF11 expression would lessen kidney fibrosis. *Gdf11*<sup>+/-</sup> mice were grossly normal and fertile with apparently normal life spans. At 8 weeks of age, baseline expression of *Gdf11* in *Gdf11*<sup>+/-</sup> mouse kidneys was ~36% of normal [ $0.363 \pm 0.0155$  ( $n = 5$ );  $P < 0.001$ ] (Figure 6C). Sirius red staining of *Gdf11*<sup>+/-</sup> mouse kidneys was significantly reduced relative to wild-type littermates, suggesting reduced collagen (Figure 6A,B). Furthermore, expression by PCR of *Col1a1* and *Col3a1* were 57% and 25% lower, respectively, in non-obstructed *Gdf11*<sup>+/-</sup> kidneys (Figure 6C). GDF11<sup>+/-</sup> mice were then subjected to UUU. At 14d, *Gdf11* expression was increased nearly 8-fold in the contralateral (uninjured) kidneys of *Gdf11*<sup>+/-</sup> mice and nearly 5-fold in wild-type mice (Figure 6F) consistent with the gene being highly induced following renal injury. Further studies will be required to understand the mechanism of the increased induction in the heterozygous mice. In contrast, *Gdf11* expression in the injured/obstructed *Gdf11*<sup>+/-</sup> kidneys remained elevated at ~2.5-fold over non-operated levels. Staining for both Sirius Red and Masson's Trichrome were reduced in the obstructed kidneys of *Gdf11*<sup>+/-</sup> versus wild-type mice (Figure 6D,E). Moreover, expression of *Col1a1*, *Col3a1*, and *Tgfb* were reduced in the ligated kidneys of *Gdf11*<sup>+/-</sup> mice vs. wild-types, while expression of *Acta2* and *Fsp1* were unchanged (Figure 6G). Thus decreased *Gdf11* expression is associated with reduced fibrosis after injury.

### GDF-11 activates fibroblasts in vitro

Renal fibrosis is mediated in part by activation of interstitial fibroblasts to myofibroblasts, and epithelial-to-myofibroblastic transition of tubular epithelial cells<sup>63-65</sup>. Thus we sought to determine the effects of recombinant GDF11 on the well-characterized renal fibroblast cell line NRK49f<sup>66</sup>. GDF11 treatment promoted a dose-dependent proliferation of NRK49f cells, although GDF11 was roughly 5–75-fold less potent than TGF- $\beta$  (Figure 7A). GDF11 also activated the myofibroblastic phenotype, as shown by induction of collagen and  $\alpha$ SMA (Figure 7B). NRK49f cells treated with GDF11 changed from a flat, hexagonal morphology and toward a more three-dimensional, spindle-shaped morphology with the formation of actin stress fibers (Figure 7C).

### GDF11-mediated EMT transition of renal tubular epithelial cells *in vitro*

The acquisition of mesenchymal markers (vimentin,  $\alpha$ SMA) in tubular epithelial cells and the reduction of renal *E-cadherin* expression observed with excess GDF11 *in vivo* indicated that GDF11 might induce EMT. We treated several renal epithelial cell lines with GDF11, including the human proximal tubular cell line HK-2<sup>67</sup>, the normal rat kidney epithelial cell line NRK52e<sup>68</sup>, and the murine intramedullary collecting duct cell line IMCD-3<sup>69</sup>. Recombinant GDF11 exposure induced a morphological change in each of these cell lines, away from the typical close-contact, cobblestone appearance of epithelial cells and toward an elongated, spindle-shaped, and scattered appearance typical of myofibroblast cells. IMCD-3 murine cells were chosen for further analysis (Figure 8A). While GDF11 treatment did not affect proliferation of IMCD-3 cells, it induced stress fiber formation and expression of fibrotic genes and mesenchymal markers. GDF11 induced expression of *Col1a1*, *Acta2*,

and *Vim*, but reduced expression of the epithelial marker E-cadherin, *Cadh1* (Figure 8B). Evidence of an EMT transition was also observed in cells grown to confluence on chamber slides. Carrier-treated cells stained strongly for E-cadherin, which was localized in thick bands corresponding to cell-cell boundaries, while GDF11-treated cells showed markedly reduced or absent E-cadherin staining (Figure 8C). Moreover,  $\alpha$ SMA and vimentin were observed at low levels in punctate granules scattered throughout the cytoplasm in carrier-treated cells, but expression of both was strongly induced in the cytoplasm of GDF11-treated IMCD-3 cells (Figure 8C). GDF11 also increased expression of the EMT mediator *Snail1*,<sup>70</sup> reduced expression of the epithelial-promoting factor *Bmp7*<sup>71</sup>, but did not affect *Tgfb* expression (Figure 8D).

To determine if the observed in vitro effects of GDF11 might be mediated by contaminating TGF $\beta$  we pre-treated IMCD-3 cells with the GDF11 binding protein follistatin, which has no known activity for TGF- $\beta$ . Follistatin inhibited GDF11 induced upregulation of  *$\alpha$ Sma* and *Vim* expression (Figure 8E). Treatment with SB43154<sup>72</sup>, an inhibitor of the receptor shared by GDF11 and TGF- $\beta$ , TGF $\beta$ R1/ALK5, preserved the cobblestone morphology of IMCD-3 cells and reduced the expression of  *$\alpha$ Sma* and *Vim* both at baseline and in response to GDF11 (Figure 8F, G). GDF11 treatment caused intracellular redistribution of SMAD2. SMAD2 was roughly distributed throughout the cytoplasm and nucleus in most untreated IMCD-3 cells. GDF11 induced SMAD2 nuclear concentration within 30 min after treatment (Figure 8H). Furthermore, addition of the SMAD3 inhibitor SIS3<sup>73</sup> significantly reduced GDF11-mediated induction of  *$\alpha$ Sma* and *Vim* (Figure 8I).

## DISCUSSION

We have shown that GDF11 is a critical regulator of adult mouse kidney fibrosis and tubular function. *Gdf11* was expressed in the adult mouse kidney and upregulated following kidney injury. Further, excess GDF11 induced kidney atrophy, fibrosis, and failure. These renal effects of GDF11 were associated with pSMAD2 and ameliorated by co-administration of the GDF11 binding protein follistatin. We also show that GDF11 expression strongly correlated with increased fibrosis; *Gdf11*<sup>+/-</sup> mice, haplo-insufficient for GDF11, had reduced baseline collagen expression and less fibrotic injury after UO. Exogenous GDF11 also induced proliferation and activation of renal fibroblasts and EMT in tubular epithelial cell cultures. These results indicate that GDF11 is increased in response to renal injury and contributes to the fibrosis that leads to progressive kidney disease.

Renal tubular epithelial cells that survive injury or insult respond by de-differentiating, losing polarity and epithelial cell markers, and often delaminating from neighboring cells. This process facilitates at least two outcomes—proliferation and epithelial re-differentiation to heal the wounded tubular epithelium and restore function, and EMT transition to form interstitial myofibroblasts that then secrete extracellular matrix and contribute to scar formation. However, this repair pathway might induce pathology when signals promoting EMT persist, reducing epithelial function and increasing matrix synthesis and deposition by tubular cells. Loss of renal function, particularly urine concentrating ability, is tightly coupled with interstitial fibrosis in human disease and experimental models<sup>74</sup>. Ureteric obstruction, for example, results in long-term urine-concentrating defects, loss of aquaporin

expression, and robust fibrosis<sup>75–77</sup>. Clinically, fibrosis is believed to be the cause of the high risk of CKD in patients who had a previous episode of AKI.<sup>78–80</sup>

Exogenous GDF11 induces expression of mesenchymal markers on tubular epithelial cells *in vivo* and *in vitro* and stimulates tubular epithelial cell proliferation *in vivo*, suggesting that GDF11 may mediate de-differentiation and proliferation of tubules in pathological conditions. Epithelial phenotype loss may promote proliferation, but also leads to dysfunction, including urine-concentrating defects through loss of differentiated states and loss of cell polarity. Alternatively and additionally, GDF11-activated SMAD proteins may mediate these effects through transcriptional regulation. GDF11 induces Snail, a zinc-finger transcription factor that represses E-cadherin expression. The combined effects of gene repression and de-differentiation, ultimately, might be responsible for loss of urine-concentrating function.

In development and adulthood, the differentiated phenotype of tubular epithelial cells is likely mediated by a balance of factors, several of which are TGF- $\beta$  family members. BMP-7 is an endogenous renal factor required for kidney organogenesis that inhibits TGF- $\beta$ -mediated EMT, promotes mesenchymal-to-epithelial transition *in vivo* and *in vitro*, and is nephroprotective in models of fibrotic kidney injury<sup>71</sup>. We show that GDF11, which is also required for kidney organogenesis<sup>20</sup> is a potent mediator of EMT *in vivo* and *in vitro*. The balance of GDF11 and BMP-7 signaling in tubular epithelial cells may determine, in part, differentiated cellular phenotype. Altered GDF11 activity also resulted in dysregulated expression of proteins involved in activating (BMP-1) or inhibiting (follistatin, BMP-7) GDF11 and related family members, indicating a complex regulatory network underlying these interrelated genes.

In sum, our results provide a potential new mediator of renal fibrosis and loss of function in renal injury. Inhibition of GDF11 activation, binding, and signaling presents a novel therapeutic target that might slow fibrosis and retard loss of function in chronic kidney disease. .

## Acknowledgments

We thank Se-Jin Lee, MD, PhD, for cell lines, mice and for assistance and advice with the study. We thank Alexandra McPherron, PhD, from NIDDK for her tissue Northern, cell line and valuable comments on the manuscript. The work was supported by funds from the IU Simon Cancer Center, the IU School of Medicine Department of Surgery and by grants to LGK (DK096167) and TZK (GM092758) and to both by the Lilly Foundation, Inc.

## Abbreviations

<b>ACVR</b>	Activin a receptor type I
<b>ALK</b>	Activin receptor like-kinase/TGF- $\beta$ receptor type I
<b><math>\alpha</math>SMA or ACTA2</b>	Alpha smooth muscle actin
<b>BUN</b>	Blood urea nitrogen
<b>BMP</b>	Bone morphogenetic protein

<b>Col</b>	Collagen
<b>EMT</b>	Epithelial to mesenchymal transition
<b>FSP1</b>	Fibroblast specific protein/S100A4
<b>FSTN</b>	Follistatin
<b>GAPDH</b>	Glyceraldehyde 2-phosphate dehydrogenase
<b>GDF</b>	Growth/differentiation factor
<b>SIS3</b>	Specific inhibitor of SMAD3
<b>TGF-<math>\beta</math></b>	Transforming growth factor-P
<b>UO</b>	Unilateral ureteric obstruction
<b>VIM</b>	Vimentin

## References

- 1 Bottinger EP. TGF-beta in renal injury and disease. *Semin Nephrol.* 2007;309–20. 2007/05/30 ed. [PubMed: 17533008]
- 2 Meng XM, Tang PM, Li J, Lan HY. TGF-beta/Smad signaling in renal fibrosis. *Front Physiol.* 2015; 6:82. [PubMed: 25852569]
- 3 Eddy AA. Overview of the cellular and molecular basis of kidney fibrosis. *Kidney Int Suppl* (2011). 2014; 4:2–8. [PubMed: 25401038]
- 4 Bottinger EP, Bitzer M. TGF-beta signaling in renal disease. *J Am Soc Nephrol.* 2002;2600–10. [PubMed: 12239251]
- 5 Zeisberg M, Kalluri R. The role of epithelial-to-mesenchymal transition in renal fibrosis. *J Mol Med.* 2004;175–81. [PubMed: 14752606]
- 6 Schnaper HW, Jandeska S, Runyan CE, Hubchak SC, Basu RK, Curley JF, et al. TGF-beta signal transduction in chronic kidney disease. *Front Biosci.* 2009;2448–65. 2009/03/11 ed.
- 7 Yamashita S, Maeshima A, Kojima I, Nojima Y. Activin A is a potent activator of renal interstitial fibroblasts. *J Am Soc Nephrol.* 2004;91–101. [PubMed: 14694161]
- 8 Maeshima A, Nojima Y, Kojima I. The role of the activin-follistatin system in the developmental and regeneration processes of the kidney. *Cytokine Growth Factor Rev.* 2001;289–98. [PubMed: 11544099]
- 9 Maeshima A, Zhang YQ, Nojima Y, Naruse T, Kojima I. Involvement of the activin-follistatin system in tubular regeneration after renal ischemia in rats. *J Am Soc Nephrol.* 2001;1685–95. [PubMed: 11461941]
- 10 Kojima I, Maeshima A, Zhang YQ. Role of the activin-follistatin system in the morphogenesis and regeneration of the renal tubules. *Mol Cell Endocrinol.* 2001;179–82.
- 11 Maeshima A, Nojima Y, Kojima I. Activin A: an autocrine regulator of cell growth and differentiation in renal proximal tubular cells. *Kidney Int.* 2002;446–54. [PubMed: 12110005]
- 12 Schneyer AL, Sidis Y, Gulati A, Sun JL, Keutmann H, Krasney PA. Differential antagonism of activin, myostatin and growth and differentiation factor 11 by wild-type and mutant follistatin. *Endocrinology.* 2008; 149:4589–95. [PubMed: 18535106]
- 13 Maeshima A, Zhang YQ, Nojima Y, Naruse T, Kojima I. Involvement of the activin-follistatin system in tubular regeneration after renal ischemia in rats. *J Am Soc Nephrol.* 2001; 12:1685–95. [PubMed: 11461941]

- 14Maeshima A, Nojima Y, Kojima I. The role of the activin-follistatin system in the developmental and regeneration processes of the kidney. *Cytokine Growth Factor Rev.* 2001; 12:289–98. [PubMed: 11544099]
- 15Kojima I, Maeshima A, Zhang YQ. Role of the activin-follistatin system in the morphogenesis and regeneration of the renal tubules. *Mol Cell Endocrinol.* 2001; 180:179–82. [PubMed: 11451589]
- 16Moon JA, Kim HT, Cho IS, Sheen YY, Kim DK. IN-1130, a novel transforming growth factor-beta type I receptor kinase (ALK5) inhibitor, suppresses renal fibrosis in obstructive nephropathy. *Kidney Int.* 2006; 70:1234–43. [PubMed: 16929250]
- 17Grygielko ET, Martin WM, Tweed C, Thornton P, Harling J, Brooks DP, et al. Inhibition of gene markers of fibrosis with a novel inhibitor of transforming growth factor-beta type I receptor kinase in puromycin-induced nephritis. *J Pharmacol Exp Ther.* 2005; 313:943–51. [PubMed: 15769863]
- 18Schiffer M, von Gersdorff G, Bitzer M, Susztak K, Bottinger EP. Smad proteins and transforming growth factor-beta signaling. *Kidney Int Suppl.* 2000; 77:S45–52. [PubMed: 10997690]
- 19Flanders KC. Smad3 as a mediator of the fibrotic response. *Int J Exp Pathol.* 2004; 85:47–64. [PubMed: 15154911]
- 20McPherron AC, Lawler AM, Lee SJ. Regulation of anterior/posterior patterning of the axial skeleton by growth/differentiation factor 11. *Nat Genet.* 1999; 22:260–4. [PubMed: 10391213]
- 21McPherron AC, Lawler AM, Lee SJ. Regulation of skeletal muscle mass in mice by a new TGF-beta superfamily member. *Nature.* 1997; 387:83–90. [PubMed: 9139826]
- 22Nakashima M, Toyono T, Akamine A, Joyner A. Expression of growth/differentiation factor 11, a new member of the BMP/TGFbeta superfamily during mouse embryogenesis. *Mechanisms of development.* 1999; 80:185–9. [PubMed: 10072786]
- 23Gamer LW, Wolfman NM, Celeste AJ, Hattersley G, Hewick R, Rosen V. A novel BMP expressed in developing mouse limb, spinal cord, and tail bud is a potent mesoderm inducer in *Xenopus* embryos. *Dev Biol.* 1999; 208:222–32. [PubMed: 10075854]
- 24Jeanplong F, Falconer SJ, Oldham JM, Maqbool NJ, Thomas M, Henneby A, et al. Identification and expression of a novel transcript of the growth and differentiation factor-11 gene. *Mol Cell Biochem.* 2014; 390:9–18. [PubMed: 24378996]
- 25Mendelsohn AR, Larrick JW. Rejuvenation of aging hearts. *Rejuvenation Res.* 2013; 16:330–2. [PubMed: 23829663]
- 26Wu HH, Ivkovic S, Murray RC, Jaramillo S, Lyons KM, Johnson JE, et al. Autoregulation of neurogenesis by GDF11. *Neuron.* 2003; 37:197–207. [PubMed: 12546816]
- 27Harmon EB, Apelqvist AA, Smart NG, Gu X, Osborne DH, Kim SK. GDF11 modulates NGN3+ islet progenitor cell number and promotes beta-cell differentiation in pancreas development. *Development.* 2004; 131:6163–74. [PubMed: 15548585]
- 28Dichmann DS, Yassin H, Serup P. Analysis of pancreatic endocrine development in GDF11-deficient mice. *Dev Dyn.* 2006; 235:3016–25. [PubMed: 16964608]
- 29Esquela AF, Lee SJ. Regulation of metanephric kidney development by growth/differentiation factor 11. *Dev Biol.* 2003; 257:356–70. [PubMed: 12729564]
- 30McNally EM. Questions and Answers About Myostatin, GDF11, and the Aging Heart. *Circ Res.* 2016; 118:6–8. [PubMed: 26837737]
- 31Sinha M, Jang YC, Oh J, Khong D, Wu EY, Manohar R, et al. Restoring systemic GDF11 levels reverses age-related dysfunction in mouse skeletal muscle. *Science.* 2014;649–52.
- 32Loffredo FS, Steinhauser ML, Jay SM, Gannon J, Pancoast JR, Yalamanchi P, et al. Growth differentiation factor 11 is a circulating factor that reverses age-related cardiac hypertrophy. *Cell.* 2013;828–39. [PubMed: 23663781]
- 33Katsimpardi L, Litterman NK, Schein PA, Miller CM, Loffredo FS, Wojtkiewicz GR, et al. Vascular and neurogenic rejuvenation of the aging mouse brain by young systemic factors. *Science.* 2014; 344:630–4. [PubMed: 24797482]
- 34Poggioli T, Vujic A, Yang P, Macias-Trevino C, Uygur A, Loffredo FS, et al. Circulating Growth Differentiation Factor 11/8 Levels Decline With Age. *Circ Res.* 2016; 118:29–37. [PubMed: 26489925]

- 35Zimmers TA, Jiang Y, Wang M, Liang TW, Rupert JE, Au ED, et al. Exogenous GDF11 induces cardiac and skeletal muscle dysfunction and wasting. *Basic Res Cardiol.* 2017; 112:48. [PubMed: 28647906]
- 36Zimmers TA, Jiang Y, Wang M, Liang TW, Rupert JE, Au ED, et al. Erratum to: Exogenous GDF11 induces cardiac and skeletal muscle dysfunction and wasting. *Basic Res Cardiol.* 2017; 112:53. [PubMed: 28721633]
- 37Egerman MA, Cadena SM, Gilbert JA, Meyer A, Nelson HN, Swalley SE, et al. GDF11 Increases with Age and Inhibits Skeletal Muscle Regeneration. *Cell Metab.* 2015; 22:164–74. [PubMed: 26001423]
- 38Rodgers BD, Eldridge JA. Reduced Circulating GDF11 Is Unlikely Responsible for Age-dependent Changes in Mouse Heart, Muscle, and Brain. *Endocrinology.* 2015 en20151628.
- 39Smith SC, Zhang X, Zhang X, Gross P, Starosta T, Mohsin S, et al. GDF11 Does Not Rescue Aging-Related Pathological Hypertrophy. *Circ Res.* 2015
- 40Zhang YH, Cheng F, Du XT, Gao JL, Xiao XL, Li N, et al. GDF11/BMP11 activates both smad1/5/8 and smad2/3 signals but shows no significant effect on proliferation and migration of human umbilical vein endothelial cells. *Oncotarget.* 2016
- 41Hinken AC, Powers JM, Luo G, Holt JA, Billin AN, Russell AJ. Lack of evidence for GDF11 as a rejuvenator of aged skeletal muscle satellite cells. *Aging Cell.* 2016
- 42Andersson O, Reissmann E, Ibanez CF. Growth differentiation factor 11 signals through the transforming growth factor-beta receptor ALK5 to regionalize the anterior-posterior axis. *EMBO Rep.* 2006; 7:831–7. [PubMed: 16845371]
- 43Oh SP, Yeo CY, Lee Y, Schrewe H, Whitman M, Li E. Activin type IIA and IIB receptors mediate Gdf11 signaling in axial vertebral patterning. *Genes Dev.* 2002; 16:2749–54. [PubMed: 12414726]
- 44Schmierer B, Hill CS. TGFbeta-SMAD signal transduction: molecular specificity and functional flexibility. *Nat Rev Mol Cell Biol.* 2007; 8:970–82. [PubMed: 18000526]
- 45Abe Y, Minegishi T, Leung PC. Activin receptor signaling. *Growth Factors.* 2004; 22:105–10. [PubMed: 15253386]
- 46Esquela AF, Lee SJ. Regulation of metanephric kidney development by growth/differentiation factor 11. *Dev Biol.* 2003;356–70. [PubMed: 12729564]
- 47Hsiao EC, Koniaris LG, Zimmers-Koniaris T, Sebald SM, Huynh TV, Lee SJ. Characterization of growth-differentiation factor 15, a transforming growth factor beta superfamily member induced following liver injury. *Mol Cell Biol.* 2000; 20:3742–51. [PubMed: 10779363]
- 48Schmittgen TD, Livak KJ. Analyzing real-time PCR data by the comparative C(T) method. *Nat Protoc.* 2008; 3:1101–8. [PubMed: 18546601]
- 49Kaufman JM, DiMeola HJ, Siegel NJ, Lytton B, Kashgarian M, Hayslett JP. Compensatory adaptation of structure and function following progressive renal ablation. *Kidney Int.* 1974; 6:10–7. [PubMed: 4419711]
- 50Hayslett JP. Functional adaptation to reduction in renal mass. *Physiol Rev.* 1979; 59:137–64. [PubMed: 220646]
- 51Al Banchaabouchi M, Marescau B, D’Hooge R, Engelborghs S, De Deyn PP. Consequences of renal mass reduction on amino acid and biogenic amine levels in nephrectomized mice. *Amino Acids.* 2000; 18:265–77. [PubMed: 10901623]
- 52Shimizu K, Yoshikawa H, Matsui M, Masuhara K, Takaoka K. Periosteal and intratumorous bone formation in athymic nude mice by Chinese hamster ovary tumors expressing murine bone morphogenetic protein-4. *Clin Orthop Relat Res.* 1994:274–80.
- 53Koniaris LG, Zimmers-Koniaris T, Hsiao EC, Chavin K, Sitzmann JV, Farber JM. Cytokine-responsive gene-2/IFN-inducible protein-10 expression in multiple models of liver and bile duct injury suggests a role in tissue regeneration. *J Immunol.* 2001; 167:399–406. [PubMed: 11418676]
- 54Zimmers TA, Davies MV, Koniaris LG, Haynes P, Esquela AF, Tomkinson KN, et al. Induction of cachexia in mice by systemically administered myostatin. *Science.* 2002; 296:1486–8. [PubMed: 12029139]
- 55Zimmers TA, McKillop IH, Pierce RH, Yoo JY, Koniaris LG. Massive liver growth in mice induced by systemic interleukin 6 administration. *Hepatology.* 2003; 38:326–34. [PubMed: 12883476]

- 56Jin X, Zimmers TA, Perez EA, Pierce RH, Zhang Z, Koniaris LG. Paradoxical effects of short- and long-term interleukin-6 exposure on liver injury and repair. *Hepatology*. 2006; 43:474–84. [PubMed: 16496306]
- 57Jin X, Zhang Z, Beer-Stolz D, Zimmers TA, Koniaris LG. Interleukin-6 inhibits oxidative injury and necrosis after extreme liver resection. *Hepatology*. 2007; 46:802–12. [PubMed: 17668886]
- 58Jin X, Zimmers TA, Zhang Z, Pierce RH, Koniaris LG. Interleukin-6 is an important in vivo inhibitor of intestinal epithelial cell death in mice. *Gut*. 59:186–96.
- 59Benny Klimek ME, Aydogdu T, Link MJ, Pons M, Koniaris LG, Zimmers TA. Acute inhibition of myostatin-family proteins preserves skeletal muscle in mouse models of cancer cachexia. *Biochemical and biophysical research communications*. 391:1548–54.
- 60Jin X, Zimmers TA, Zhang Z, Pierce RH, Koniaris LG. Interleukin-6 is an important in vivo inhibitor of intestinal epithelial cell death in mice. *Gut*. 2010; 59:186–96. [PubMed: 19074180]
- 61Walker RG, Poggioli T, Katsimpardi L, Buchanan SM, Oh J, Wattrus S, et al. Biochemistry and Biology of GDF11 and Myostatin: Similarities, Differences, and Questions for Future Investigation. *Circ Res*. 2016; 118:1125–42. [PubMed: 27034275]
- 62Schneyer A, Sidis Y, Xia Y, Saito S, del Re E, Lin HY, et al. Differential actions of follistatin and follistatin-like 3. *Mol Cell Endocrinol*. 2004; 225:25–8. [PubMed: 15451564]
- 63Zeisberg M, Kalluri R. The role of epithelial-to-mesenchymal transition in renal fibrosis. *J Mol Med*. 2004; 82:175–81. [PubMed: 14752606]
- 64Kalluri R, Neilson EG. Epithelial-mesenchymal transition and its implications for fibrosis. *J Clin Invest*. 2003; 112:1776–84. [PubMed: 14679171]
- 65Liu Y. Epithelial to mesenchymal transition in renal fibrogenesis: pathologic significance, molecular mechanism, and therapeutic intervention. *J Am Soc Nephrol*. 2004; 15:1–12. [PubMed: 14694152]
- 66Yang J, Dai C, Liu Y. Hepatocyte growth factor suppresses renal interstitial myofibroblast activation and intercepts Smad signal transduction. *Am J Pathol*. 2003; 163:621–32. [PubMed: 12875981]
- 67Docherty NG, O’Sullivan OE, Healy DA, Murphy M, O’Neill AJ, Fitzpatrick JM, et al. TGF-beta1-induced EMT can occur independently of its proapoptotic effects and is aided by EGF receptor activation. *Am J Physiol Renal Physiol*. 2006; 290:F1202–12. [PubMed: 16368739]
- 68Fan JM, Ng YY, Hill PA, Nikolic-Paterson DJ, Mu W, Atkins RC, et al. Transforming growth factor-beta regulates tubular epithelial-myofibroblast transdifferentiation in vitro. *Kidney Int*. 1999; 56:1455–67. [PubMed: 10504497]
- 69Ivanova L, Butt MJ, Matsell DG. Mesenchymal transition in kidney collecting duct epithelial cells. *Am J Physiol Renal Physiol*. 2008; 294:F1238–48. [PubMed: 18322023]
- 70Boutet A, De Frutos CA, Maxwell PH, Mayol MJ, Romero J, Nieto MA. Snail activation disrupts tissue homeostasis and induces fibrosis in the adult kidney. *EMBO J*. 2006; 25:5603–13. [PubMed: 17093497]
- 71Zeisberg M, Shah AA, Kalluri R. Bone morphogenic protein-7 induces mesenchymal to epithelial transition in adult renal fibroblasts and facilitates regeneration of injured kidney. *J Biol Chem*. 2005; 280:8094–100. [PubMed: 15591043]
- 72Laping NJ, Grygielko E, Mathur A, Butter S, Bomberger J, Tweed C, et al. Inhibition of transforming growth factor (TGF)-beta1-induced extracellular matrix with a novel inhibitor of the TGF-beta type I receptor kinase activity: SB-431542. *Mol Pharmacol*. 2002; 62:58–64. [PubMed: 12065755]
- 73Jinnin M, Ihn H, Tamaki K. Characterization of SIS3, a novel specific inhibitor of Smad3, and its effect on transforming growth factor-beta1-induced extracellular matrix expression. *Mol Pharmacol*. 2006; 69:597–607. [PubMed: 16288083]
- 74Bohle A, Mackensen-Haen S, von Gise H. Significance of tubulointerstitial changes in the renal cortex for the excretory function and concentration ability of the kidney: a morphometric contribution. *Am J Nephrol*. 1987; 7:421–33. [PubMed: 3439552]
- 75Li C, Wang W, Kwon TH, Isikay L, Wen JG, Marples D, et al. Downregulation of AQP1, -2, and -3 after ureteral obstruction is associated with a long-term urine-concentrating defect. *Am J Physiol Renal Physiol*. 2001; 281:F163–71. [PubMed: 11399657]

- 76Li C, Wang W, Knepper MA, Nielsen S, Frokiaer J. Downregulation of renal aquaporins in response to unilateral ureteral obstruction. *Am J Physiol Renal Physiol.* 2003; 284:F1066–79. [PubMed: 12517734]
- 77Shi Y, Li C, Thomsen K, Jorgensen TM, Knepper MA, Nielsen S, et al. Neonatal ureteral obstruction alters expression of renal sodium transporters and aquaporin water channels. *Kidney Int.* 2004; 66:203–15. [PubMed: 15200427]
- 78Ishani A, Xue JL, Himmelfarb J, Eggers PW, Kimmel PL, Molitoris BA, et al. Acute kidney injury increases risk of ESRD among elderly. *J Am Soc Nephrol.* 2009; 20:223–8. [PubMed: 19020007]
- 79Lo LJ, Go AS, Chertow GM, McCulloch CE, Fan D, Ordonez JD, et al. Dialysis-requiring acute renal failure increases the risk of progressive chronic kidney disease. *Kidney Int.* 2009; 76:893–9. [PubMed: 19641480]
- 80Lafrance JP, Miller DR. Defining acute kidney injury in database studies: the effects of varying the baseline kidney function assessment period and considering CKD status. *Am J Kidney Dis.* 2010; 56:651–60. [PubMed: 20673605]

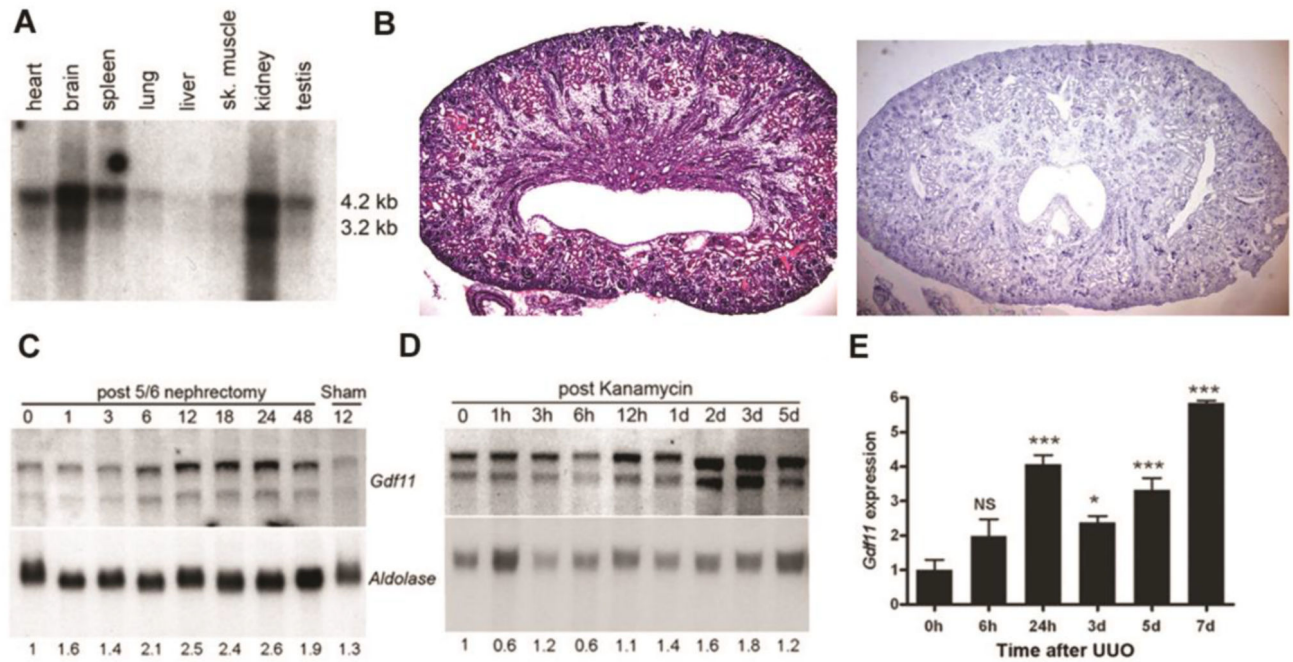


**Figure 1. Expression of *Gdf11* in normal adult kidney, in tubular epithelial cells and after kidney injury**

(A) Northern blot analysis of 2  $\mu$ g twice poly(A)-selected mRNA shows two transcripts hybridizing to a cDNA probe corresponding to the C-terminal domain of *Gdf11* in various adult mouse tissues. (B) H&E staining (left) and in situ hybridization for *Gdf11* (right) in neonatal kidney shows expression in distal tubules, cortical collecting ducts, and medullary rays. (C) Northern blot analysis of *Gdf11* expression in 10  $\mu$ g total RNA from the remnant kidney at the number of hours indicated after removal of one kidney and resection of 2/3 of the other, and from (D) kidneys after kanamycin treatment at the indicated hours (h) or days (d) after injury. *Gdf11* was normalized to *aldolase* expression as a loading control. (E) *Gdf11* levels in total RNA isolated from ligated kidneys after unilateral ureteric obstruction (UUO) at the indicated hours (h) or days (d) after injury were measured by quantitative real-time RT-PCR (qRT-PCR) and normalized to *Gapdh* in this and all subsequent figures. *Gdf11* levels are plotted relative to sham-operated kidney at time 0 ( $n = 3-5$  mice each). \* $P < 0.05$ , \*\* $P < 0.01$ , \*\*\* $P < 0.001$

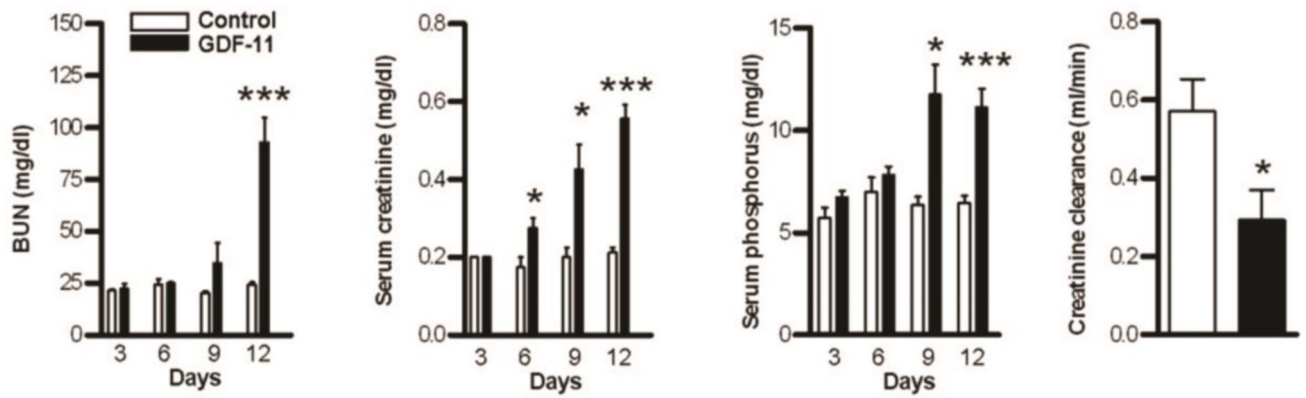


**Figure 2. GDF11 administration induces renal failure**

Blood urea nitrogen (BUN), serum creatinine, and phosphorus, along with creatinine clearance in control (white bars) and GDF11-treated (black bars) mice euthanized on the indicated day after injection ( $n = 4-12$  mice each). \* $P < 0.05$ , \*\*\* $P < 0.001$

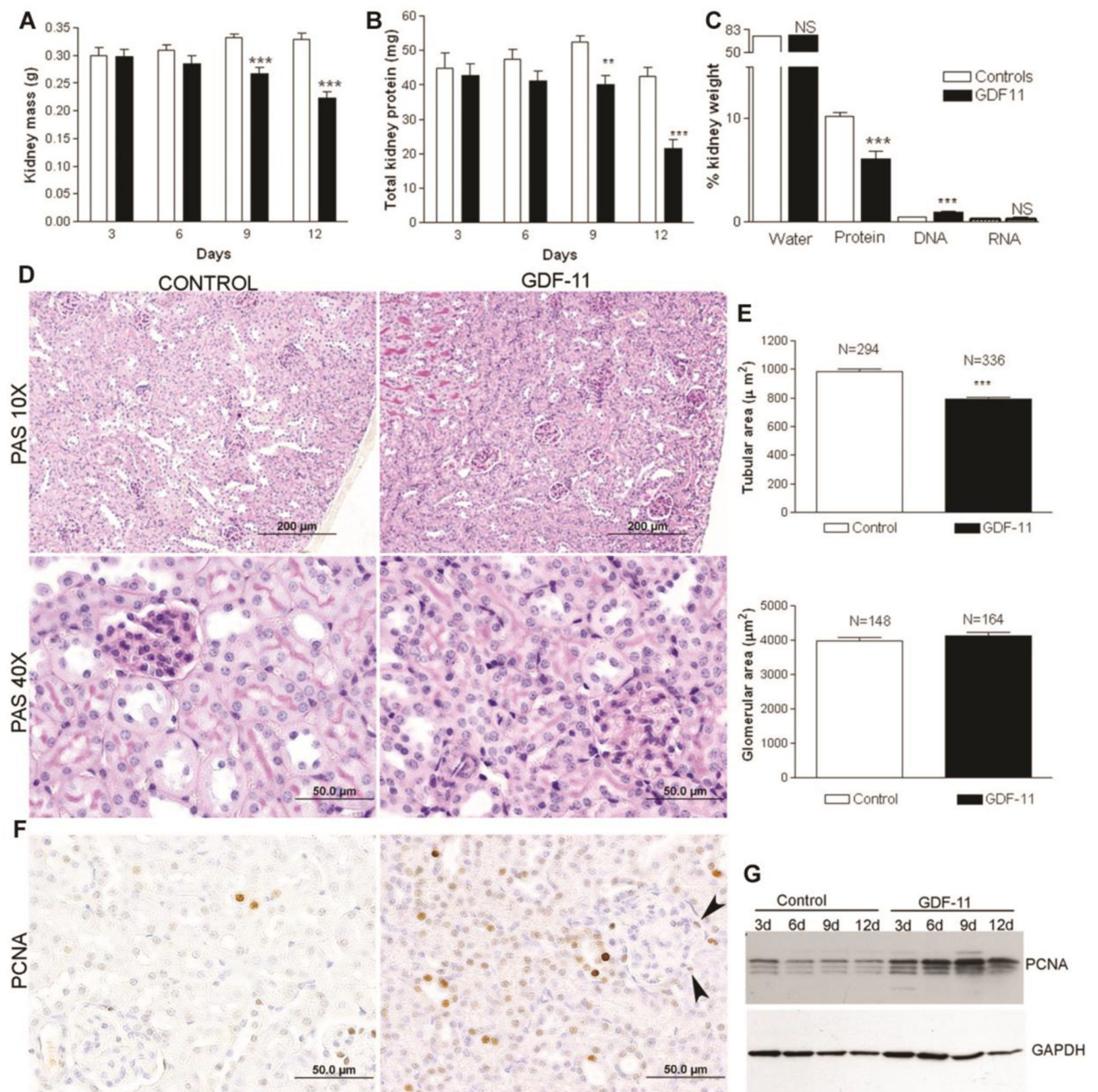


**Figure 3. GDF11 administration induces kidney protein wasting and epithelial cell and interstitial cell proliferation**

(A) Mouse kidney mass, (B) total kidney protein, and (C) percentage water, protein, DNA and RNA content measured in control and GDF11-treated mice at the indicated time after injection ( $n = 4-12$  per group). (D) PAS staining and (E) morphometric analysis for tubular area and glomerular area in control and GDF11 treated mice. (F) Immunohistochemical staining for PCNA shows positive nuclei in tubules and interstitial cells but not glomeruli. (G) Western blot for PCNA in kidney extracts from control and GDF11-treated mice at the indicated day (d) post injection. \* $P < 0.05$ , \*\* $P < 0.01$ , \*\*\* $P < 0.001$

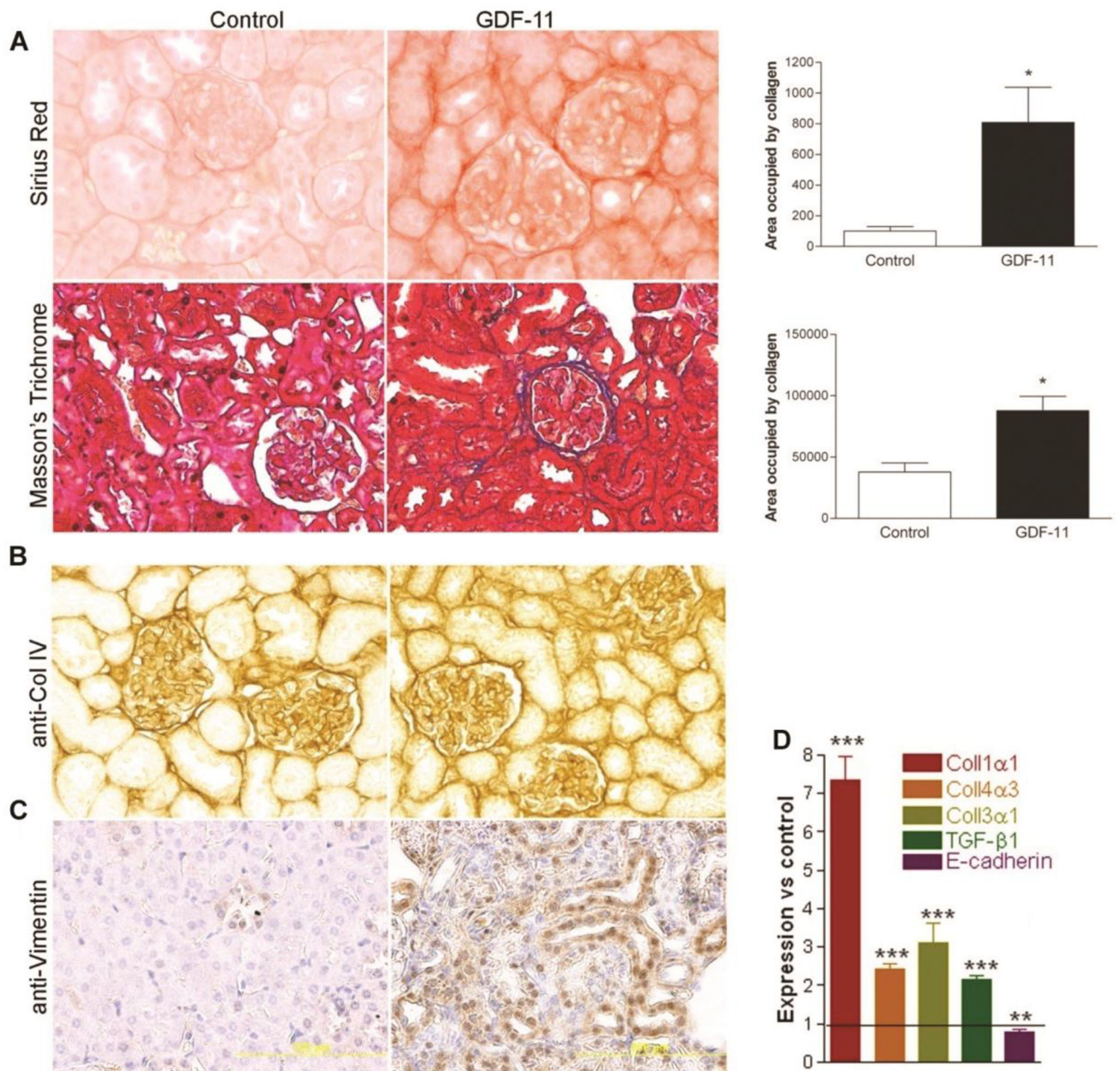


**Figure 4. Systemic GDF11 treatment induces renal fibrosis by 12 days**

(A) Histological evidence of fibrotic change in kidneys from GDF-11-treated mice, including Sirius red staining (top panel) and quantification, Masson's Trichrome staining (lower panel) and quantification of each (right). (B) Immunohistochemical staining for collagen IV and (C) for vimentin increased in kidney sections from GDF11-treated mice. (D) qPCR analysis of expression of *Coll1 $\alpha$ 1*, *Coll4 $\alpha$ 3*, *Coll3 $\alpha$ 1*, *Tgfb1*, and *Cdh1* mRNA in GDF-11-treated kidneys at 12 d, normalized to *Gapdh* and expressed relative to control-treated kidney from the same day (n = 4 per group). \* $P < 0.05$ , \*\* $P < 0.01$ , \*\*\* $P < 0.001$

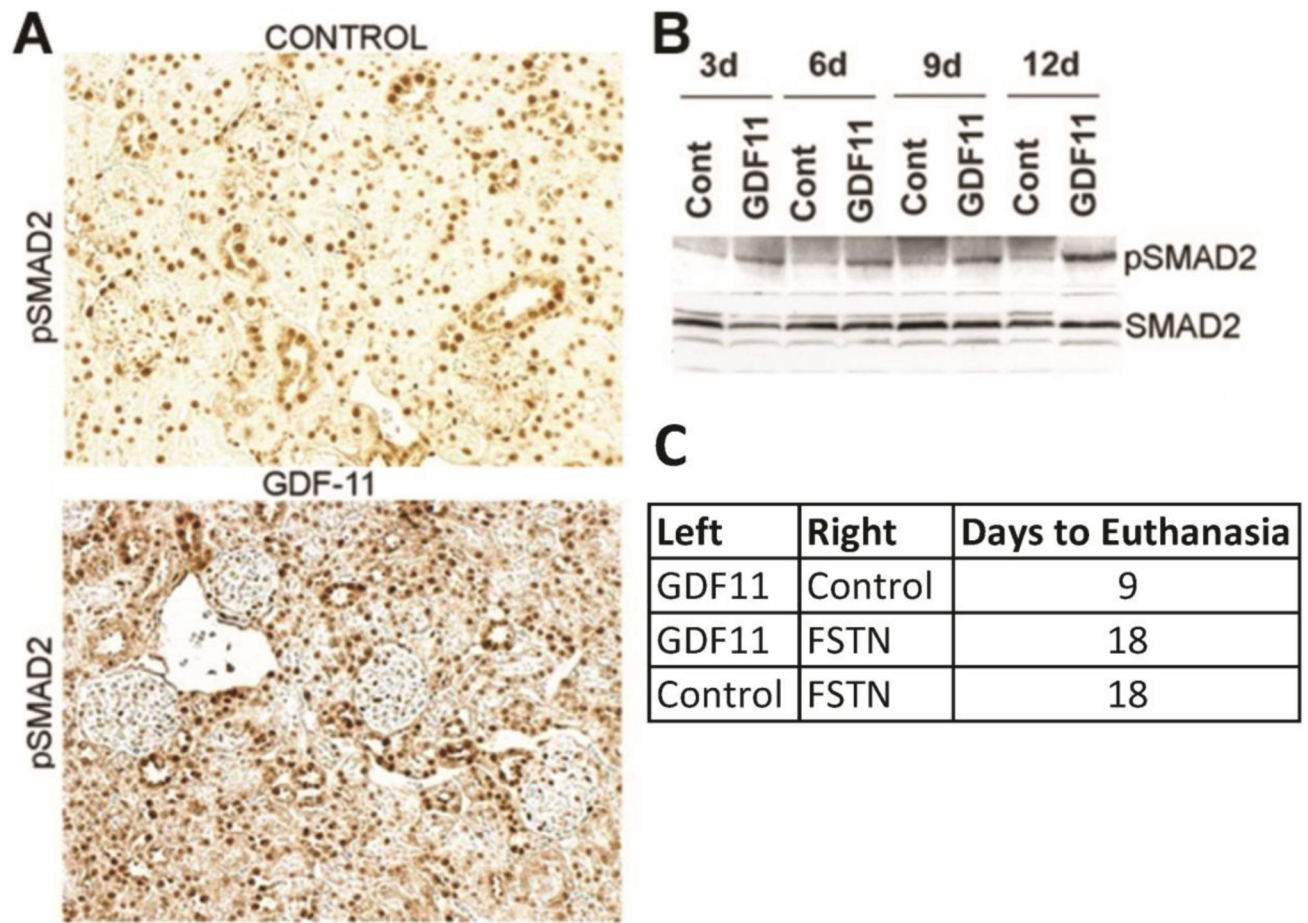


**Fig 5. GDF11 treatment activated kidney pSMAD2 and was blocked by co-administration of Follistatin**

(A) Immunohistochemistry of pSMAD2 in kidney sections of outer cortex from control and GDF11-treated mice at 12 d. (B) Western blots of SMAD2 and pSMAD2 on kidney extracts from control or GDF11-treated mice at the indicated day (d) after injection. (C) Survival of mice dual-injected in opposite legs with CHO-control/CHO-follistatin cells ( $n = 6$ ), CHO-control/CHO-GDF11 ( $n = 6$ ), or CHO-follistatin/CHO-GDF11 cells ( $n = 5$ ). In this trial, CHO-GDF11 mice were euthanized when they became moribund 9d after injection. CHO-control/CHO-follistatin-treated mice were euthanized due to tumor burden at 18d. Mice bearing both CHO-follistatin/CHO-GDF11 cells survived to 18 d and were euthanized.  $P < 0.0001$

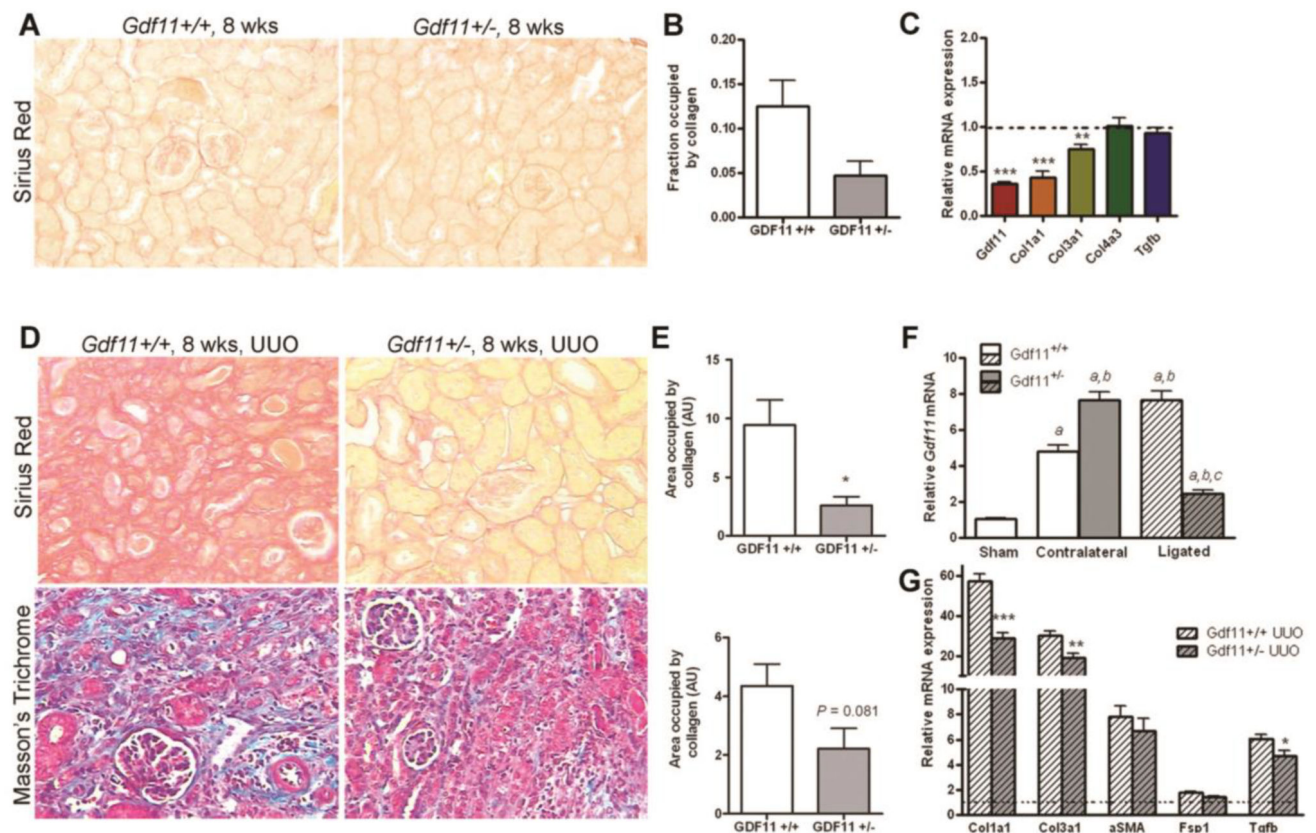


### Figure 6. Reduced fibrosis in normal and ligated *Gdf11*<sup>+/-</sup> kidneys

(A). Representative images and (B) quantification of Sirius Red collagen staining of kidney sections from 8-week-old *Gdf11*<sup>+/+</sup> and *Gdf11*<sup>+/-</sup> mice. (C) QPCR analysis of *Gdf11*, *Col1a1*, *Col3a1*, *Col4a3*, and *Tgfb1* expression in 8-week-old *Gdf11*<sup>+/+</sup> and *Gdf11*<sup>+/-</sup> mice (n = 4 per group). (D) Representative images and (E) quantification of Sirius Red collagen staining and Masson's Trichrome staining of ligated kidneys 14 d after unilateral ureteric obstruction (UUO) in 8-week-old *Gdf11*<sup>+/+</sup> and *Gdf11*<sup>+/-</sup> mice. (F) QPCR analysis of *Gdf11* mRNA induction in ligated and contralateral (non-ligated) kidneys from 8-week-old *Gdf11*<sup>+/-</sup> and *Gdf11*<sup>+/+</sup> mice after UUO. (G) QPCR analysis of *Col1a1*, *Col3a1*, *Tgfb1*, *Acta2*, and *Fsp1* expression in the ligated kidneys of *Gdf11*<sup>+/+</sup> and *Gdf11*<sup>+/-</sup> mice after UUO (n = 4 per group). \**P* < 0.05, \*\**P* < 0.01, \*\*\**P* < 0.001

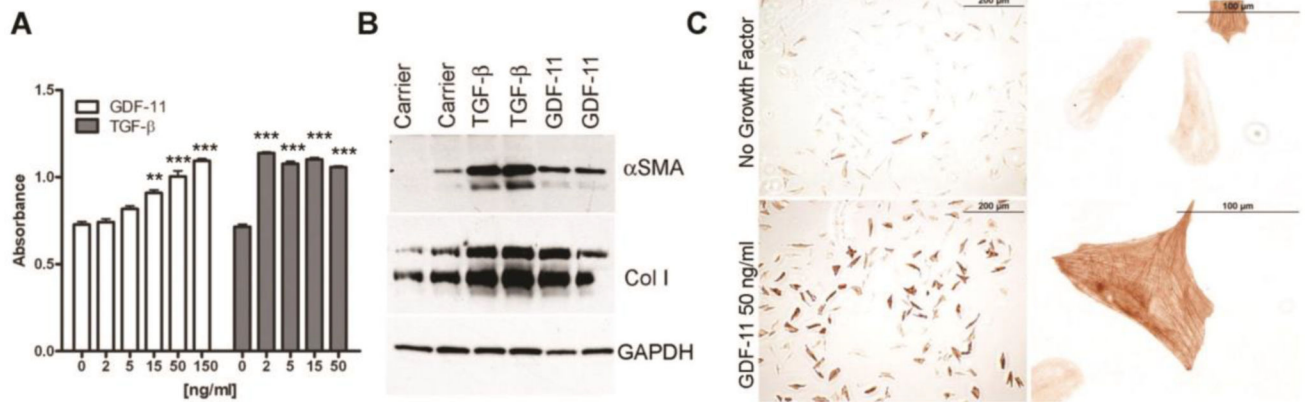


**Figure 7. GDF11 induces activation and proliferation of renal fibroblasts**

(A) MTT dye reduction assay of NRK49f murine renal fibroblasts after 5 d of culture with the indicated dose of recombinant GDF11 (white) or TGF-β (grey). (B) Western blot analysis of αSMA and collagen I (Col I) in extracts from NRK49f cells starved for 48 h before treatment with recombinant TGF-β or GDF11 for 18 h. GAPDH is a loading control. (C) Immunohistochemistry for αSMA in NRK49f cells grown in chamber slides and treated for 48 h with carrier containing no growth factor or with 50 ng/mL GDF11. \*\* $P < 0.01$ , \*\*\* $P < 0.001$ .

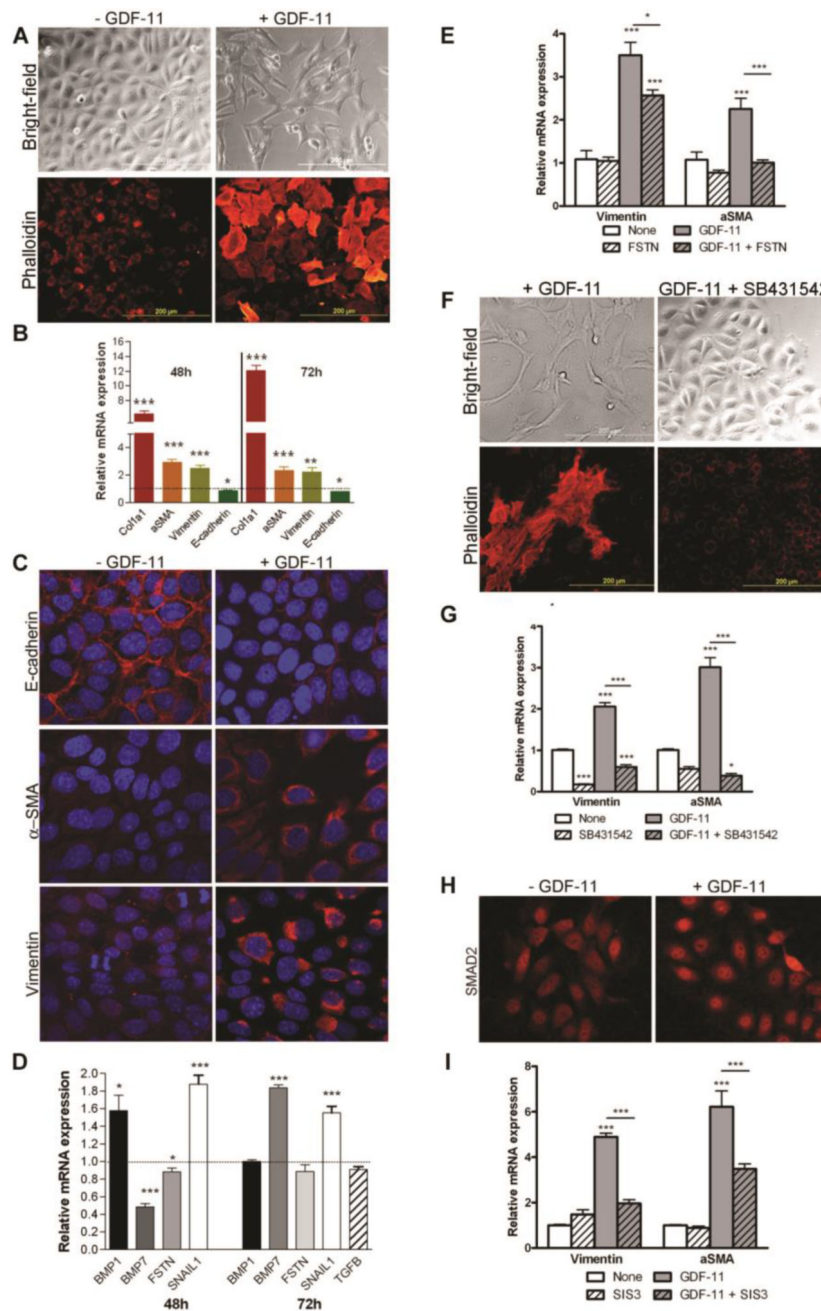


**Figure 8. Exogenous GDF11 induces epithelial-to-mesenchymal transition in murine intramedullary collecting duct cells**

(A) Bright-field images of IMCD-3 cells after 72 hours of growth on plastic culture dishes, and phalloidin staining showing formation of stress fibers and altered morphology in IMCD-3 cells after 48 h of growth on chamber slides. Cells were either not treated or treated with 50 ng/mL recombinant GDF11. (B) QPCR analysis of *Col1a1*, *Acta2*, *Vim*, and *Cdh1* expression in IMCD-3 cells treated with 50 ng/mL recombinant GDF11 for 48 h or 72 h. Results are normalized to *Gapdh* and expressed relative to control-treated cells. (C) Confocal micrographs of IMCD-3 cells treated with control or 50 ng/mL recombinant GDF11 for 96 h and immunofluorescently stained for E-cadherin (top panel),  $\alpha$ -SMA (middle panel), and

vimentin (bottom panel) (all red) and counterstained with DAPI (blue). (D) QPCR analysis of *Snail1*, *Tgfb*, *Bmp1*, *Bmp7*, and *Fstn* mRNA in IMCD-3 cells treated with GDF11 for 48 h or 72 h. (E) qRT-PCR analysis of vimentin and  $\alpha$ SMA expression in control IMCD-3 cells or those treated with follistatin (FSTN) and/or GDF11. (F) Bright-field and phalloidin-stained images of morphological changes in IMCD-3 cells after treatment with GDF11 and/or the ALK5 inhibitor SB431542. (G) QPCR analysis of *Vim* and  $\alpha$ *Sma* expression in control IMCD-3 cells or those treated with GDF11 and/or SB431542. (H) Nuclear localization of SMAD2 by indirect immunofluorescence staining of IMCD-3 cells starved for 18 h and then stimulated with 50 ng/ml GDF11 or control for 30 min. (I) qRT-PCR analysis of *Vim* and  $\alpha$ *Sma* expression in control IMCD-3 cells or those treated with GDF11 and/or the SMAD3 inhibitor SIS3. All qRT-PCR results are normalized to *Gapdh* and expressed relative to control-treated cells. \* $P < 0.05$ , \*\* $P < 0.01$ , \*\*\* $P < 0.001$

Table 1

Renal function in control and GDF-11-treated mice 12 d after injection

	Control		GDF11		P
	Mean ± SEM	N	Mean ± SEM	N	
Body weight (G)	25.56 ± 0.48	13	19.08 ± 0.42	8	0.0001
Urine output (mL/24 h)	1.85 ± 0.12	8	8.75 ± 0.99	8	0.0001
Water intake (mL/24 h)	6.37 ± 0.32	8	14.88 ± 1.16	8	0.0001
Blood urea nitrogen (mg/dL)	24.20 ± 1.28	15	92.94 ± 11.81	16	0.0001
Serum creatinine (mg/dL)	0.21 ± 0.01	16	0.56 ± 0.04	16	0.0001
Serum sodium (mmol/L)	138.00 ± 2.28	8	140.30 ± 3.37	6	NS
Serum potassium (mmol/L)	4.60 ± 0.35	4	7.42 ± 0.79	4	0.05
Serum phosphorus (mg/dL)	6.44 ± 0.36	16	11.09 ± 0.94	16	0.0001
Serum osmolality (mOsm/kg H <sub>2</sub> O)	273.60 ± 4.10	8	297.8 ± 8.87	5	0.05
Creatinine clearance (mL/min)	0.57 ± 0.08	4	0.29 ± 0.08	4	0.05
Urine osmolality (mOsm/kg H <sub>2</sub> O)	3225 ± 218.5	4	449 ± 48.07	4	0.0001
Urine creatinine (mg/24 h)	1.61 ± 0.17	4	2.71 ± 0.67	4	NS
Urine total protein (mg/24 h)	6.89 ± 0.32	4	2.60 ± 0.57	4	0.0001

**Table 2**

## Primers for qRT-PCR analysis

<i>18S rRNA</i>	Forward	5'- CATGTGGTGTGAGGAAAGCAG-3'
	Reverse	5'- TCTTGACTGTCGTGGGTTCTG-3'
<i>Acta2</i> (αSMA)	Forward	5'- ACTGGGACGACATGGAAAAG-3'
	Reverse	5'- CATCTCCAGAGTCCAGCACA-3'
<i>Bmp1</i>	Forward	5'- CAGGCAACCGCATGTTCTT-3'
	Reverse	5'- GTGGGATGCCTGGAAACCT-3'
<i>Bmp7</i>	Forward	5'- TGTGGCAGAAAACAGCAGCA-3'
	Reverse	5'- TCAGGTGCAATGATCCAGTCC-3'
<i>Coll o</i>	Forward	5'-AAAGGCTGGAGAGCGA-3'
	Reverse	5'- AGCAGGACCTGGGGGA-3'
<i>Col3a1</i>	Forward	5'- TGGTCCTCAGGGTGTAAGG-3'
	Reverse	5'- GTCCAGCATCACCTTTTGGT-3'
<i>Col4a3</i>	Forward	5'- CCCAGCCAGTCCATTATAGAAT-3'
	Reverse	5'- CAGCGAAGCCAGCCAGAA-3'
<i>Cadh1</i> (E-cadherin)	Forward	5'- AAGAAGACCAGGACTTTGATTTGAGCCAGCTGC-3'
	Reverse	5'- TTCAGAACCACTGCCCTCGTAATCGAACACCAACAG-3'
<i>Gapdh</i>	Forward	5'-TGCACCACCAACTGCTTAG-3'
	Reverse	5'-GGATGCAGGGATGATGTTTC-3'
<i>Tgfb1</i>	Forward	5'- GCAACATGTGGAAGTCTACCAGA-3'
	Reverse	5'- GACGTCAAAAGACAGCCACTCA-3'
<i>Vim</i> (Vimentin)	Forward	5'- ATGCGTGAGATGGAAGAGAATTTGC-3'
	Reverse	5'- TTATTCAAGGTCATCGTGATGCTGAGA-3'